Supplemental information

Liver Mitochondrial Cristae Organizing Protein MIC19 Promotes Energy Expenditure and Pedestrian Locomotion by Altering Nucleotide Metabolism

Jee Hyung Sohn, Beste Mutlu, Pedro Latorre-Muro, Jiaxin Liang, Christopher F. Bennett, Kfir Sharabi, Noa Kantorovich, Mark Jedrychowski, Steven P. Gygi, Alexander S. Banks, Pere Puigserver

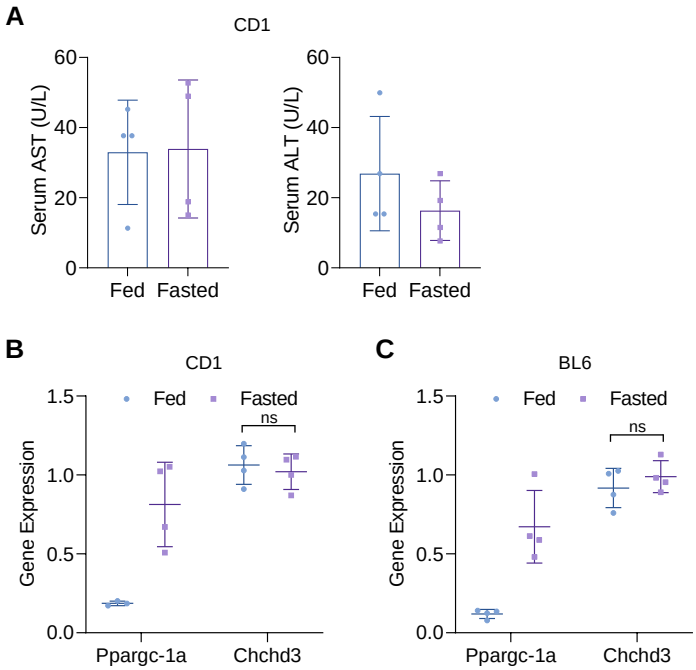

Figure S1. Fasting does not induce liver toxicity and hepatic Chchd3 expression, related to Figure 1. (A) Serum AST and ALT levels in fed vs. fasted CD-1 mice (n=4). (B and C) *Ppargc-1a* and *Chchd3* mRNA levels normalized to 36B4 control gene in fed vs. fasted livers in CD-1 and BL6 (n=3~4). All data represented as mean±SD. *p* value by Student's t-test (A-C). n represents the number of biological replicates.

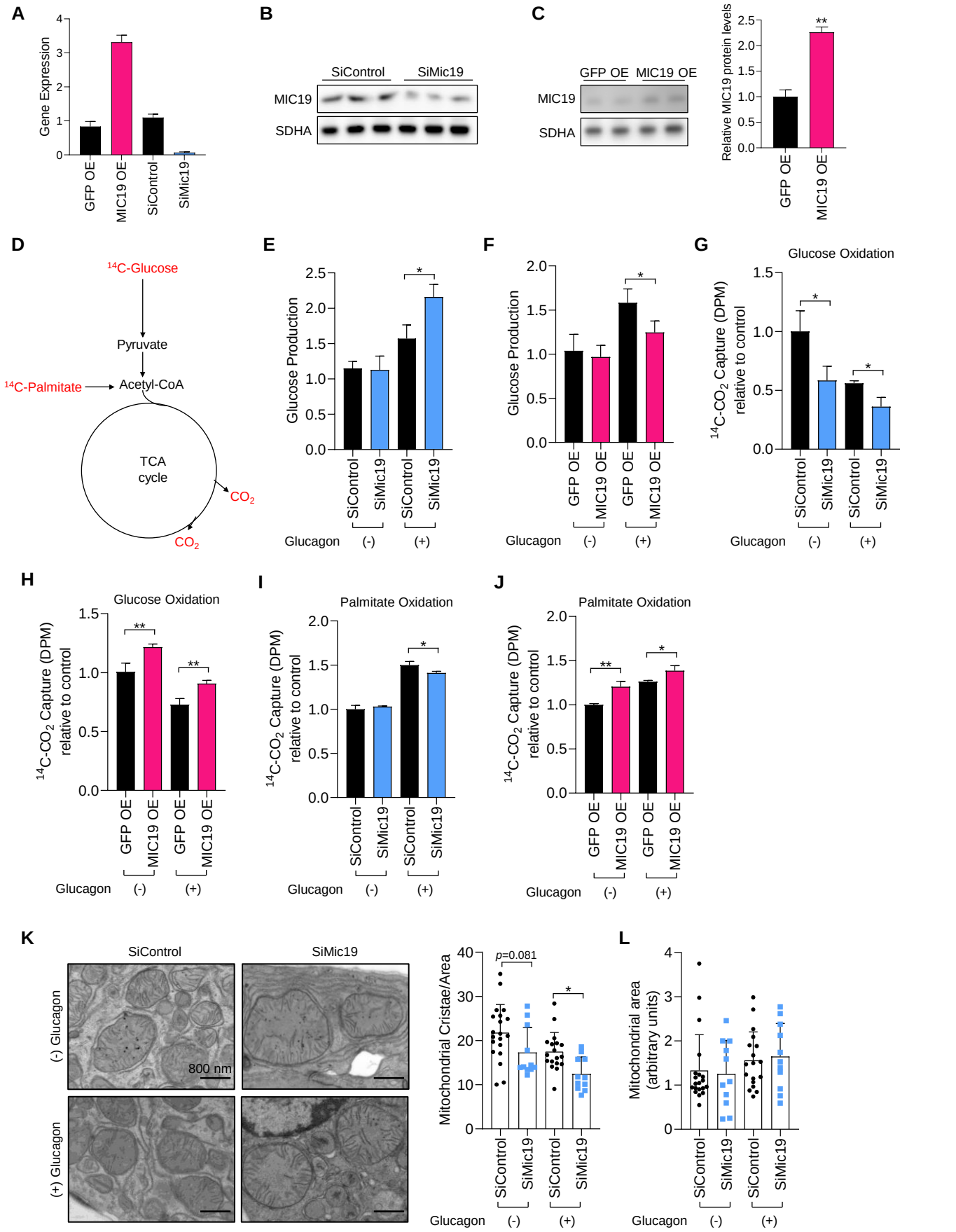
A
Gene Expression
GFP OE
MIC19 OE
SiControl
SiMic19
B
SiControl
SiMic19
MIC19
SDHA
C
GFP OE
MIC19 OE
MIC19
SDHA
Relative MIC19 protein levels
D
14C-Glucose
Pyruvate
14C-Palmitate
Acetyl-CoA
TCA cycle
CO2
CO2
E
Glucose Production
Glucagon
(-)
(+)
F
Glucose Production
G
Glucose Oxidation
14C-CO2 Capture (DPM) relative to control
H
Glucose Oxidation
I
Palmitate Oxidation
J
Palmitate Oxidation
K
SiControl
SiMic19
(-) Glucagon
(+) Glucagon
800 nm
Mitochondrial Cristae/Area
p=0.081
L
Mitochondrial area (arbitrary units)

Figure S2. Modulation of MIC19 in BL6 primary hepatocytes reveals metabolic changes in glucose metabolism and fatty acid oxidation, related to Figure 3. Chchd3 gene expression normalized to 36B4 in primary hepatocytes comparing SiControl vs. SiMic19 and GFP Overexpression (OE) vs. MIC19 OE (n=3). (B and C) MIC19 protein levels in primary hepatocytes comparing SiControl vs. SiMic19 and GFP OE vs. MIC19 OE (n=2). (D) Description of the pathways for the assays that measure oxidation of ^{14}C-palmitate or ^{14}C-glucose through the TCA cycle, which leads to the release of ^{14}C-CO_2. (E and F) Hepatic Glucose Production in primary hepatocytes from pyruvate and lactate with or without 100 nM Glucagon stimulation, in siControl vs. SiMic19 or GFP vs. MIC19 OE (n=4~6). (G and H) Measurement of ^{14}C-CO2 released by the oxidation of ^{14}C-glucose with or without 100 nM Glucagon stimulation, in siControl vs. SiMic19 (p=0.01 for SiControl to SiMic19 or GFP vs. MIC19 OE (n=3). (I and J) Measurement of ^{14}C-CO_2 released by the oxidation of ^{14}C-palmitate with or without 100 nM Glucagon stimulation, in siControl vs. SiMic19 or GFP vs. MIC19 OE (n=3). (K and L) Cristae abundance and mitochondria total area in primary hepatocytes upon siMic19 treatment (n=11~20 images). All data represented as mean±SD. **p*< 0.05, ***p*< 0.01 by Student's t-test (C-J) or by two-way ANOVA followed by Tukey post hoc test (K, L). n represents the number of biological replicates.

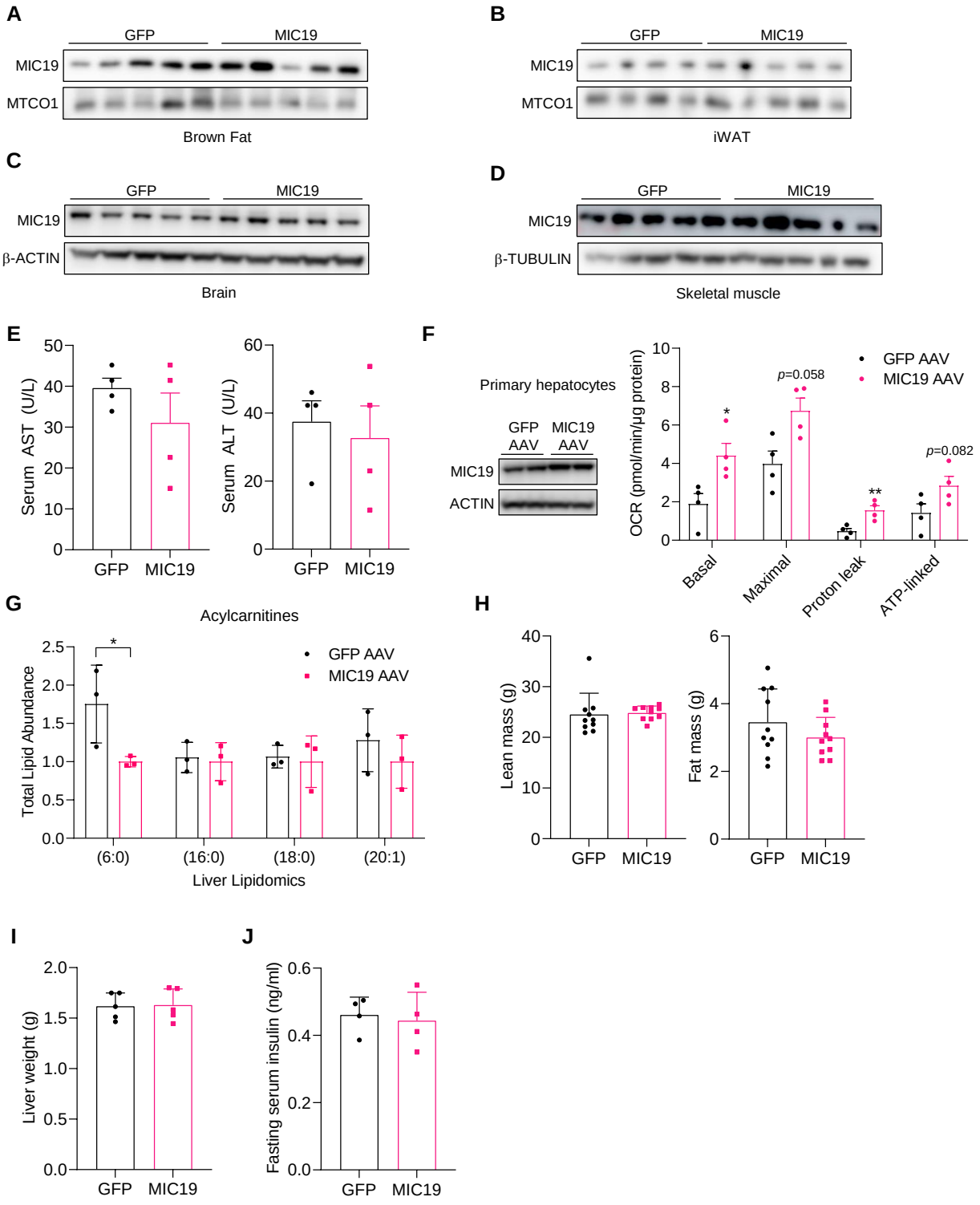

Figure S3. Phenotypes of MIC19 overexpressing mice are analyzed, related to Figure 3. (A-D) Western Blot against MIC19 protein in total lysates from brown fat, inguinal white adipose tissue (iWAT), brain, and skeletal muscle of GFP vs. MIC19 AAV animals (n=4~5). (E) Serum AST and ALT levels in fasted GFP vs. MIC19 AAV mice. (F) Oxygen consumption rates in primary hepatocytes after GFP or MIC19 AAV transduction. (G) Acylcarnitine levels in GFP vs. MIC19 AAV livers quantified by lipidomics. (H-J) Lean and fat mass, liver weight, and fasting insulin level in serum of GFP vs. MIC19 AAV mice. Data represented as mean±SD (G-J) or as mean±SEM (E, F). *p< 0.05, **p< 0.01 by Student's t-test (E-J). n values indicated in the figures refer to biological replicates.

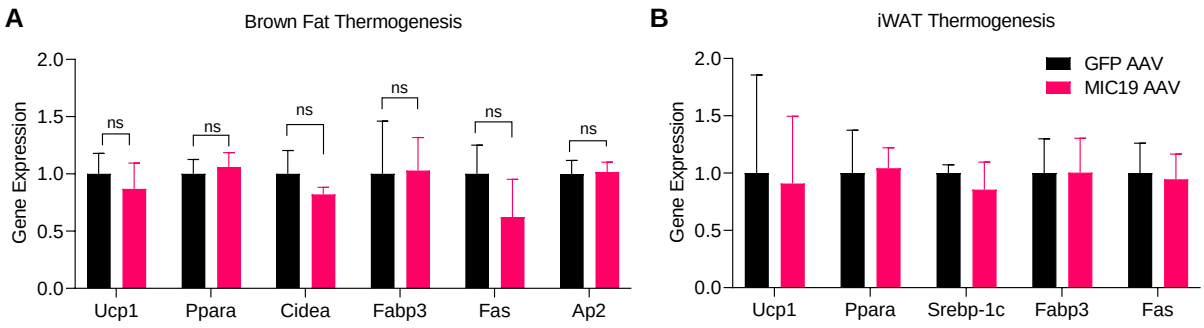

Figure S4. Thermogenic gene expression remains the same in adipose tissue in GFP vs. MIC19 AAV animals, related to Figure 5. (A and B) Gene expression for thermogenic markers in BAT (n=4) and iWAT (n=3) normalized to 36B4. All data represented as mean±SD. *p* value by Student's t-test. n represents the number of biological replicates.

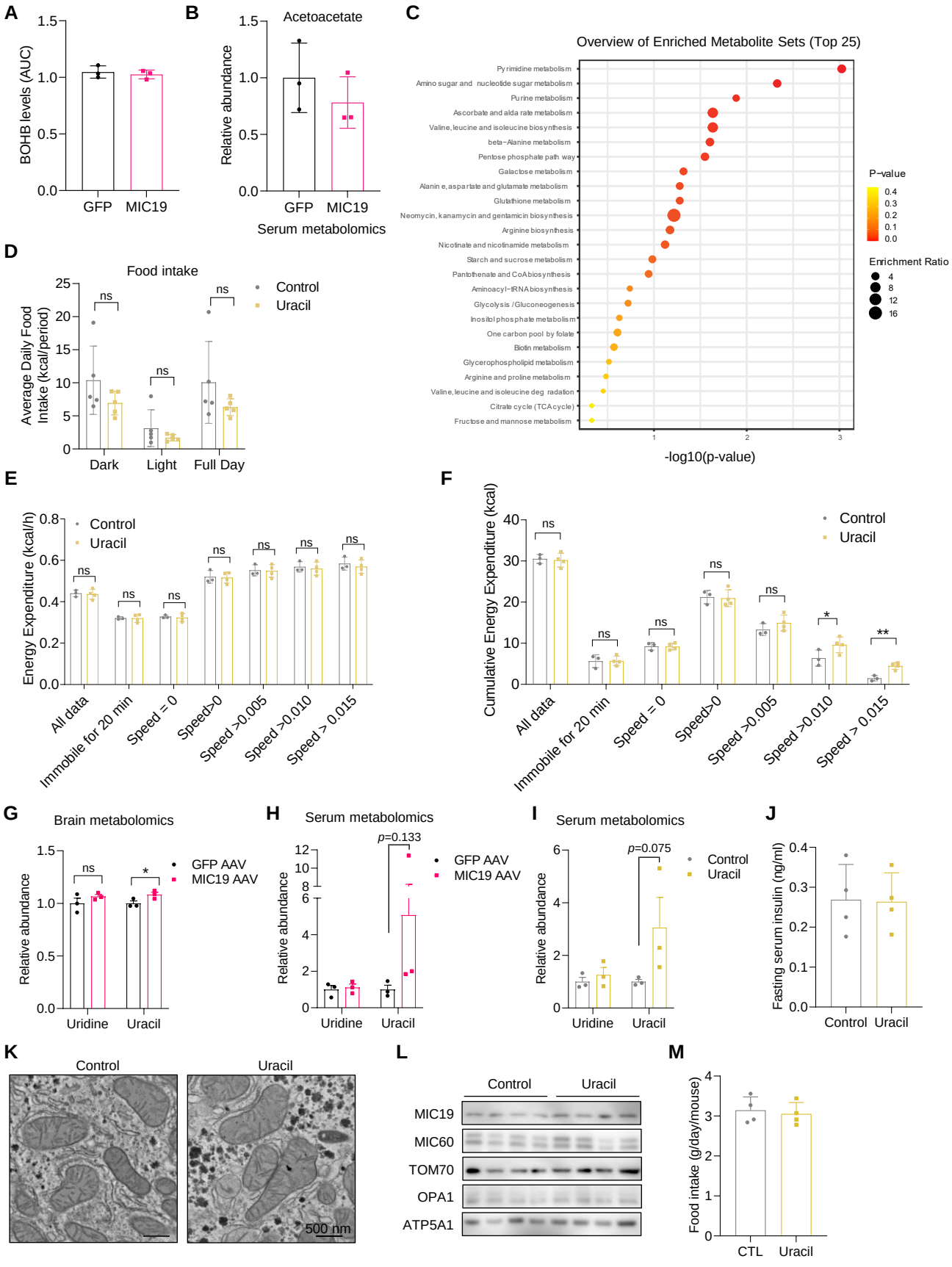
A
BOHB levels (AUC)
GFP
MIC19
B
Acetoacetate
Relative abundance
Serum metabolomics
C
Overview of Enriched Metabolite Sets (Top 25)
Pyrimidine metabolism
Amino sugar and nucleotide sugar metabolism
Purine metabolism
Ascorbate and aldarate metabolism
Valine, leucine and isoleucine biosynthesis
beta-Alanine metabolism
Pentose phosphate pathway
Galactose metabolism
Alanine, aspartate and glutamate metabolism
Glutathione metabolism
Neomycin, kanamycin and gentamicin biosynthesis
Arginine biosynthesis
Nicotinate and nicotinamide metabolism
Starch and sucrose metabolism
Pantothenate and CoA biosynthesis
Aminoacyl-tRNA biosynthesis
Glycolysis / Gluconeogenesis
Inositol phosphate metabolism
One carbon pool by folate
Biotin metabolism
Glycerophospholipid metabolism
Arginine and proline metabolism
Valine, leucine and isoleucine degradation
Citrate cycle (TCA cycle)
Fructose and mannose metabolism
-log10(p-value)
P-value
Enrichment Ratio
D
Food intake
Average Daily Food Intake (kcal/period)
Control
Uracil
Dark
Light
Full Day
E
Energy Expenditure (kcal/h)
All data
Immobile for 20 min
Speed = 0
Speed>0
Speed >0.005
Speed >0.010
Speed > 0.015
F
Cumulative Energy Expenditure (kcal)
G
Brain metabolomics
Relative abundance
GFP AAV
MIC19 AAV
Uridine
Uracil
H
Serum metabolomics
p=0.133
I
Serum metabolomics
p=0.075
J
Fasting serum insulin (ng/ml)
K
Control
Uracil
500 nm
L
MIC19
MIC60
TOM70
OPA1
ATP5A1
M
Food intake (g/day/mouse)
CTL

Figure S5. Liver metabolomics identifies pyrimidine nucleotide uracil as regulator of locomotion, related Figure 6. (A and B) BHOB and acetoacetate levels in the serum of GFP vs. MIC19 AAV mice. (C) Top 25 enriched metabolites from the metabolomics analysis of GFP vs. MIC19 AAV livers (n=3). (D) Average Daily Food Intake of mice with or without uracil supplementation (0.1% in drinking water). (E) Mean energy expenditure at certain speeds (m/s) in animals with or without uracil supplementation. (F) Cumulative energy expenditure at certain speeds (m/s) in animals with or without uracil supplementation. (G and H) Relative abundance of uridine and uracil in the brains and serum of GFP vs. MIC19 AAV mice from a metabolomics experiment (I) Relative abundance of uridine and uracil in serums of mice with or without 1% uracil supplementation (J-L) Fasting insulin level in serum, mitochondrial cristae morphology in the liver, and mitochondrial protein expression in isolated liver mitochondria of mice with or without 1% uracil supplementation. (M) Food intake of mice on HFD supplemented with uracil (0.1% in drinking water). Data represented as mean±SD (A, B, D-F,J, M) or as mean±SEM (G-I). *p< 0.05, **p< 0.01 by Student's t-test (A, B, D-J, M). n values indicated in the figures refer to biological replicates.

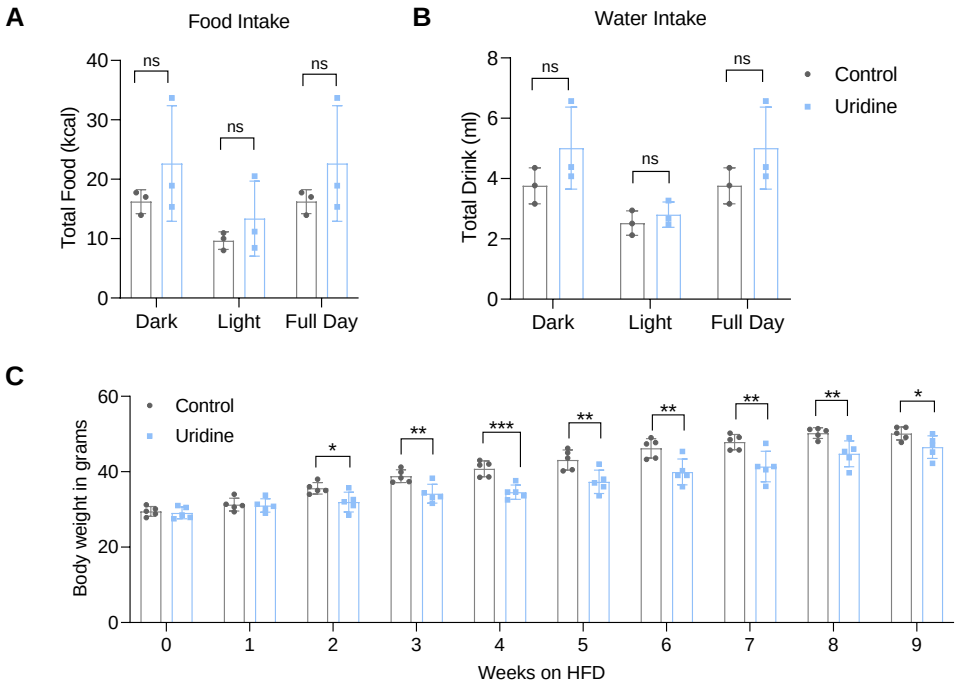

Figure S6. Uridine, precursor for uracil, protects against diet-induced obesity, related to Figure 7. Metabolic parameters were measured in mice with or without uridine supplementation (3% drinking water) (A and B) Food and water intake (n=3). (C) Body weight of mice on HFD supplemented with uridine (n=5). All data represented as mean±SD. *p< 0.05, **p< 0.01, ***p< 0.001 by Student's t-test (A, B, D-J, M). n represents the number of biological replicates.